VIP Porphyrin Analogues

DOI: 10.1002/anie.200900496

Tetraazuliporphyrin Tetracation**

*Natasza Sprutta, Stanisław Maćkowiak, Marzena Kocik, Ludmiła Szterenberg, Tadeusz Lis, and Lechosław Latos-Grażyński**

Dedicated to Professor Emanuel Vogel

Modifications of a porphyrin core that involve the replacement of one[1–6] or two[7–15] of the nitrogen atoms by CH units have led to a new class of macrocycles known as carbaporphyrinoids, which have interesting properties both in terms of their aromaticity and their potential ability to bind metal ions. An extension of the mono- and dicarbaporphyrinoid concept to tri- and tetracarbaporphyrinoids is a logical and long-awaited development in the carbaporphyrinoid field.[16–20] In fact, when exploring this area, one is inspired by the pioneering work of Vogel and co-workers, who introduced a whole family of aromatic tetraheteroporphyrin dications that preserve the porphyrin-like skeleton but with the nitrogen atoms replaced by four oxygen, sulfur, or selenium atoms.[16,21–24] Importantly, this approach, the aim of which was to treat porphyrins from the perspective of the annulene chemist, allows the incorporation of two CH_2 and two −CH=CH− units, which act as inner and outer bridges, into the parent [18]annulene (**1**). This modification results in the bridged annulene, which corresponds to the aromatic tetracyclopentadienic hydrocarbon **2**.[16,17]

Compound **2** can be regarded as the parent structure of porphyrins or heteroporphyrins (Scheme 1).[16,17] This compound, which has been named quatyrin,[19,20] and its oxidized derivative dehydroquatyrin (**3**) have not been reported to date, although the importance of **2** to the fields of both annulenes and porphyrins has been highlighted.[20] Consequently, the synthesis of quatyrin and any compound that contains a quatyrin-containing frame is a fascinating goal at the intersection of carbaporphyrinoid, annulene, cyclophane, and carbocation chemistry.

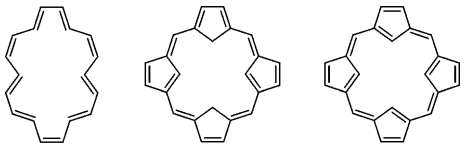

1 **2** **3**

Scheme 1. Structures of [18]annulene (**1**), quatyrin (**2**), and dehydroquatyrin (**3**).

Herein, we report the synthesis and characterization of the tetraaryltetraazuliporphyrin tetracation **5** (Scheme 2). The macrocycle contains (formally) the dehydroquatyrin **3** skeleton, which can be derived in a straightforward manner from the hypothetical 5,10,15,20-tetraaryldehydroquatyrin **4** by the fusion of four tropylium cations to the perimeter of the macrocycle.

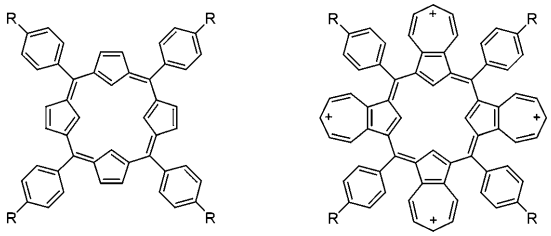

4 **5**

Scheme 2. 5,10,15,20-tetraaryldehydroquatyrin (**4**) and the 5,10,15,20-tetraazuliporphyrin tetracation **5**.

The first step of the synthesis of the tetraaryltetraazuliporphyrin tetracation **5** requires the formation of 5,10,15,20-tetraaryltetraazuliporphyrinogen (5,10,15,20-tetraarylcalix(4)azulene) **6**, which was obtained from a modified synthesis of tetratolyl-21,23-dithia- and tetratolyl-21,23-dioxadiazuliporphyrinogen.[14,15] This method relies on the known suitability of azulene as a substrate for Rothemund-type condensations, which is well demonstrated in the syntheses of calix(4)azulene ((1.1.1.1)((1,3)-azulenophane),[20] calix(4)-2-methoxyazulene, ((1.1.1.1)((1,3)-2-methoxyazulenophane),[25] and 5,10,15,20-tetraarylazuliporphyrin.[26]

To synthesize **6**, we used the Lindsey-type one-pot reaction of azulene and arylaldehyde (1:1 molar ratio), which was carried out in dichloromethane and catalyzed by $BF_3{\cdot}Et_2O$ (Scheme 3). 4-methylbenzaldehyde, benzaldehyde, and 4-methoxybenzaldehyde were tested, and remarkable overall yields of 5,10,15,20-tetraaryltetraazuliporphyrinogen **6** were obtained in each case (97% for **6a**, 61% for **6b**, and 40% for **6c**). Porphyrinogens were invariably obtained as a mixture of stereoisomers, which were distinguished by considering the orientation of the meso-aryl groups with respect

[*] Dr. N. Sprutta, S. Maćkowiak, M. Kocik, Dr. L. Szterenberg, Prof. T. Lis, Prof. L. Latos-Grażyński
Department of Chemistry, University of Wrocław
14 F.Joliot-Curie St., 50-383 Wrocław (Poland)
Fax: (+48) 71-328-2348
E-mail: llg@wchuwr.pl
Homepage: http://www.chem.uni.wroc.pl/llg/

[**] Financial support from the Ministry of Science and Higher Education (Grant PBZ-KBN-118/T09/2004) is acknowledged. DFT calculations were carried out at the Supercomputer Centers of Poznań and Wrocław.

Supporting information for this article is available on the WWW under http://dx.doi.org/10.1002/anie.200900496.

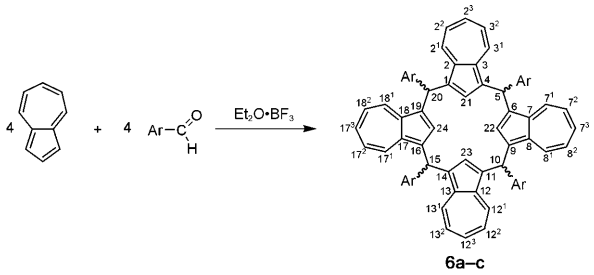

Scheme 3. Synthesis of 5,10,15,20-tetraaryltetraazuliporphyrinogen (**6a**: Ar = *p*-Tol, **6b**: Ar = Ph, **6c**: Ar = OMePh).

to the $(C_{meso})_4$ plane (α up, β down; the effective symmetry arising from conformational flexibility is given in parentheses): αααα, **6-1** (C_{4v}), ααββ, **6-2** (C_{2h}), αααβ, **6-3** (C_s), and αβαβ, **6-4** (C_{2v}).

The macrocycles were separated by fractional crystallization from acetone and/or column chromatography, and the steroisomers were identified by using a combination of X-ray crystallography and NMR spectroscopy. By comparing the ^{1}H NMR spectra of the pure isomers (Figure 2) with that of the isomeric mixture, it was established that **6-1** and **6-2** were the major condensation products for all investigated meso substituents. Compounds **6a-1** and **6a-2** have been characterized by X-ray crystallography (Figure 1).[27] The arrangement of the azulene rings in **6a-2** leads to a chairlike conformation in the solid state. Two opposing rings are moderately bent away from the $(C_{meso})_4$ plane, whereas the dihedral angle between the two other azulene rings and the $(C_{meso})_4$ plane is 87.6°. The stereoisomer **6a-1** reveals also a similar arrangement of a single couple of opposing azulene rings and a canted couple of two others. In contrast to **6a-2**, two other tropyl moieties are located on the same side of the $(C_{meso})_4$ plane, and four meso-tolyl groups create a cavity surrounded by a picket-fence-like structure. The bond lengths and angles of azulene fragments in both structures are similar to those of nonmodified azulene.

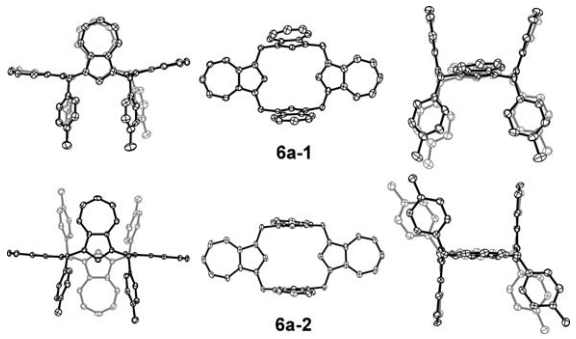

Figure 1. X-ray crystal structures of **6a-1** and **6a-2**. Hydrogen atoms, meso-*p*-tolyl groups in the central projections, and solvent molecules are omitted for clarity. Fragments pointing into the paper are shown in gray. Thermal ellipsoids are shown at the 50 % probability level.

All the ^{1}H NMR resonances of **6a-1** and **6a-2** were unambiguously assigned by symmetry analysis (Figure 2). The spectroscopic identification of the minor component **6a-3** was also possible because its unique C_s symmetry is reflected by a specific ^{1}H NMR pattern. In each case, the signals of the azulene rings are in regions expected of a porphyrinogen-like structure devoid of macrocyclic conjugation. The fast exchange between the two limiting conformers of **6a-1**, each characterized by a C_{2v} solid-state symmetry, affords dynamic equivalence in the ^{1}H NMR spectrum, which corresponds to an effective C_{4v} symmetry (Figure 3).

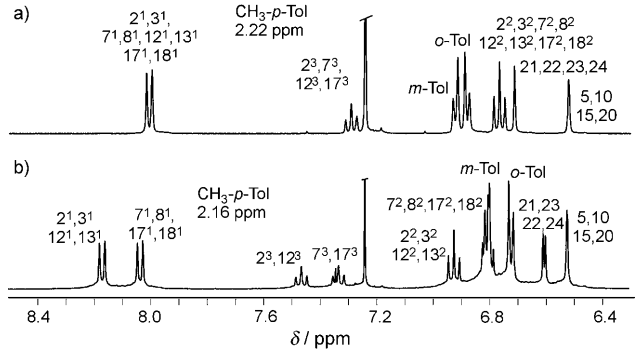

Figure 2. ^{1}H NMR spectra of a) **6a-1** ($CDCl_3$, 298 K) and b) **6a-2** ($CDCl_3$, 298 K).

Figure 3. Dynamic exchange to afford an effective C_{4v} symmetry of **6a-1** (structures generated by molecular mechanic calculations).

The transformation of tetrazuliporphyrinogens into the tetraazuliporphyrin tetracation **5** requires, at least in theory, a stepwise removal of four hydride groups from the meso positions, and is accompanied by rehybridization from sp^3 to sp^2. Thus, the oxidation of **6-1** or **6-2** can be formally split into four subsequent steps, where each step corresponds to the formation of monomeric (1-azulenyl)phenylmethyl cations. In fact, the formation of highly stable azulene analogues of the triphenylmethyl cation, including the di(1-azulenyl)phenylmethyl cation, from the corresponding hydroderivatives by hydride abstraction with 2,3-dichloro-5,6-dicyano-1,4-benzoquinone (DDQ) has been described in detail.[28–30]

The oxidation of **6a-2** with DDQ in dichloromethane with different amounts of oxidant (molar ratio from 1:0.25 to 1:8), which was followed by using ^{1}H NMR spectroscopy and mass spectrometry, typically afforded an inseparable mixture of products. A detailed analysis of the ^{1}H NMR spectra showed that the reaction proceeded by the gradual formation of a monocationic form $[(\mathbf{6a\text{-}2})-H]^+$, followed by a dication $[(\mathbf{6a\text{-}2})-2H]^{2+}$, and eventually stopped at the trication $[(\mathbf{6a\text{-}2})-3H]^{3+}$ stage. The oxidation of tetraazuliporphyrinogen **6a-2**, which was carried out using DDQ (1:8 molar ratio) in dichloromethane but followed by the crucial addition of $HBF_4{\cdot}Et_2O$, yielded the desired tetracation **5a**. Significantly,

the identical tetracationic species has been generated by using the other porphyrinogen **6a-1**.

When compound **6a-2** is oxidized to **5a**, significant changes are seen in its electronic spectra (Figure 4). The signals in the UV/Vis spectrum of **6a-2** (Figure 4, inset), which

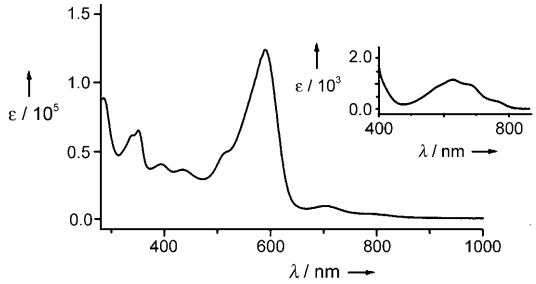

Figure 4. UV/Vis spectra of **5a** (CH_2Cl_2, 298 K) and **6a-2** (inset, CH_2Cl_2, 298 K).

bears the characteristic features of free azulene, are replaced by a set of intense bands in the visible region with the most intense signal located at 588 nm. The spectrum of **5a** resembles those of azulene-containing methylium salts.[31–33]

The mass spectrum (ESI) of **5a** shows four major sets of peaks that correspond to the presence of the parent tetracation **5a** and its one- ($[\mathbf{5a}+e^-]^{3+}$) two- ($[\mathbf{5a}+2e^-]^{2+}$), and three-electron ($[\mathbf{5a}+3e^-]^{+}$) reduction products that are formed in the ionization procedure. In each set, which correspond to *m*/4, *m*/3, *m*/2, and *m*, respectively, the isotopomer peaks are consistently separated by 0.25, 0.33, 0.5, and 1 units, respectively. The identity of **5a** was confirmed by ^{1}H and ^{13}C NMR spectroscopy. The remarkable simplification of the ^{1}H NMR of **5a** (Figure 5a) compared to the starting porphyrinogens **6a-2** (Figure 2b) is consistent with the effective D_{4h} symmetry of the tetraazuliporphyrin tetracation. The spectrum consists of single sets of the azulene and meso-*p*-tolyl resonances, and is distinguished by the downfield shift (11.34 ppm) of the H(21) resonance.

Three major canonical contributions (Scheme 4) can be considered to account for the electronic structure of the tetraazuliporphyrin tetracation. In two structures (**5** and **5′**), the positive charge is located at the tropylium units, which allows an inner antiaromatic conjugation arising from imprinted [16]annulene or dehydroquatyrin (**3**). The third structure (**5″**) involves the splitting of the macrocycle into a set of four monocarbocations at the meso bridges. The ^{1}H NMR results for **5a** are atypical, but the chemical shifts are consistent with a non-aromatic structure (Figure 5), which allows us to treat **5** and **5′** as the rather minor, albeit aesthetically tempting, contributors. The macrocyclic aromatic ring current is essentially absent The H(21) resonance of **5a** is shifted downfield compared to that of **6a-2**, which is in agreement to some degree with the considered effect of macrocyclic paratropicity. In fact, this observation may be related to increasing charge confined to the macrocyclic

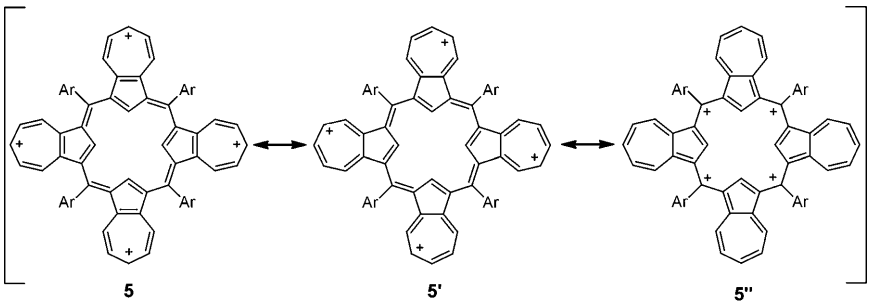

Scheme 4. Canonical structures of **5**.

porphyrin-like frame. Interestingly, once the donor properties of the meso-aryl *p*-substituents increase, the chemical shift of the inner hydrogen markedly decreases following the series 11.57 ppm for **5b**, 11.34 ppm for **5a**, and 10.39 ppm for **5c**, whereas the other resonances retain their positions.

A combination of HMBC, HMQC, and ADEQUATE-(1,1) correlations allowed the unambiguous identification of all the carbon resonances of **5a** (Table 1). Changes in the ^{13}C chemical shifts can be used to evaluate the charge distribution in carbocations, because the positively charged carbon atoms are strongly deshielded, as expected for a carbocationic structure.[34,35] Remarkably, the ^{13}C resonances of the carbon atoms that constitute the macrocyclic frame show noteworthy downfield shifts, which are characteristic of tetraazuliporphyrinogen, with the largest effects seen for the C(5), C(2), C(21), and C(2^2) atoms (Table 1).

We realized that understanding the perimeter reactivity of **5** is essential when considering potential functionalizations or applications for the reversible binding of anions or weak nucleophiles. The ^{1}H NMR titration of **5a** with D_2O (Figure 5) showed a systematic decrease of the resonances of **5a**, which was accompanied by the appearance of a new set of resonances assigned to the $[(\mathbf{5a}+OH^-)]^{3+}$ adduct, where the hydroxy unit is linked to one of the meso positions. The

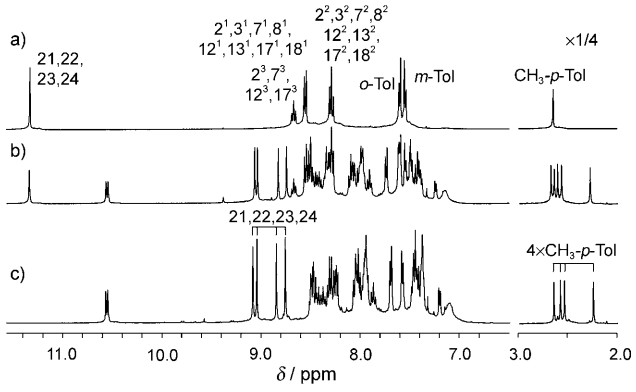

Figure 5. ^{1}H NMR titration of **5a** with D_2O (CD_3CN, 298 K): a) **5a**, b) mixture of **5a** and $[(\mathbf{5a}+OH^-)]^{3+}$, and c) $[(\mathbf{5a}+OH^-)]^{3+}$.

Table 1: ^{13}C chemical shifts and charges for **5a** and **6a**-1.

Position	Chemical shift [ppm]		NPA charges[a]	
	6a-1	**5a**	**6a-1**	**5a**
1	132.2	141.0	−0.058	−0.106
2	135.6	160.4	−0.038	+0.008
5	41.4	177.0	−0.293	+0.141
21	139.4	168.2	−0.192	−0.129
2^1	133.4	143.3	−0.159	−0.138
2^2	121.5	144.9	−0.267	−0.184
$2^{3'}$	137.3	150.8	−0.191	−0.140
o-Tol	128.7	136.1	−0.230	−0.182
m-Tol	128.7	132.6	−0.229	−0.223
p-Tol	135.2	153.2	−0.036	+0.077
ipso	142.3	136.2	−0.003	−0.135
CH_3-*p*-Tol	21.1	22.7	−0.698	+0.008

[a] Natural population analyses (NPA) were performed at the B3LYP/6-31G** level.

process can be reversed by the addition of $HBF_4{\cdot}Et_2O$ to the solution. The monoaddition lowers the symmetry of the species, thus rendering the four azulene units inequivalent. Consequently, the number of resonances in the spectrum of $[(\mathbf{5a}+OH^-)]^{3+}$ is four times that of **5a**, as clearly illustrated by the presence of four singlet signals assigned to the H(21), H(22), H(23), and H(24) atoms (Figure 5c). The four *p*-methyl singlet signals of the meso-*p*-tolyl group are divided in two subsets, which reflects the oxidation or hybridization status at the adjacent meso carbon atom. The *p*-tolyl groups attached to carbenium centers give rise to *p*-methyl resonances at approximately 2.6 ppm, similar to the spectrum of **5a**, whereas the single tolyl group bound to a tetrahedral carbon atom gives rise to the characteristic signal at 2.2 ppm, which was observed for porphyrinogen **6a-2**. The parallel experiment in which CD_3OD was used as a nucleophile yielded the analogous $[(\mathbf{5a}+CD_3O^-)]^{3+}$ adduct.

DFT studies were used to visualize the suggested structure of the tetraazuliporphyrin tetracation (Figure 6). The macrocycle of **5a** is severely distorted into a saddle shape, which resembles the sterically strained tetraphenyltetrabenzoporphyrin.[36] Each azulene ring is displaced up and down alternately, and the *p*-tolyl rings are rotated into the macrocycle plane to minimize contacts between the substituents. Adjacent azulene rings in **5a** are tilted with an angle of 112.6°, where the dihedral angles between two opposite rings are 76.4° and 67.5°, respectively. Each individual azulene ring is planar. The optimized bond lengths of azulene moiety resemble those found by X-ray crystallography for **6a-1** and **6a-2**. The trigonal geometry around the meso carbon atom resembles that of triphenylmethyl cation.[37]

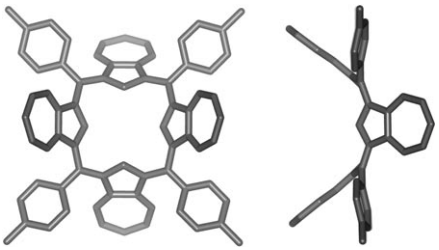

Figure 6. The DFT-optimized structure of **5a**.

The computed charges of **5a** and the charge differences (Δcharge) for DFT optimized structures of tetraazuliporphyrinogen **6a-1** and the tetraazuliporphyrin tetracation **5a** are summarized in Table 1 and Figure 7. The positive charge is significantly localized at the meso positions of **5a**. All but two (C(1) and C_{ipso}) sp^2 carbon atoms of **5a** gain a positive charge because of the oxidation of **6a-1**, with the largest effect seen for the C(5), C(21), and C(2^2) atoms.

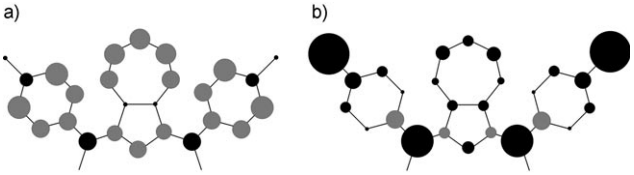

Figure 7. a) Computed NPA-derived charges for **5a** and b) Δcharges relative to parent **6a-1** (the area of circle is roughly proportional to the magnitude of the corresponding value, black circles represent positive charge and gray circles negative charge).

In summary, the standard condensation of azulene and arylaldehyde followed by oxidation provides straightforward access to the tetraazuliporphyrin tetracation, which is the first species to incorporate an intriguing dehydroquatyrin motif into its molecular structure. Although these investigations have been strongly motivated by the search for tetracarbaporphyrinoids, we have readily appreciated that, because of its peculiar nature, this molecule links several seemingly distant fields of exploration by addressing some issues of cyclophane, annulene, polyarene, azulene carbocation, or calixarene chemistry. This easily accessible organic tetracation may exhibit interesting properties as a host for small molecules or anions, as it plays the role of a preorganized, rigid, and highly charged squarelike macrocyclic receptor. Considering the perceived importance of azulene-stabilized cations in the design of electronic materials, the tetracationic building block may be regarded as a potential alternative for conductive or semiconductive applications.

Received: January 26, 2009
Published online: March 31, 2009

Keywords: annulenes · azulenes · carbaporphyrinoids · cyclophanes · porphyrinoids

[1] P. J. Chmielewski, L. Latos-Grażyński, K. Rachlewicz, T. Głowiak, *Angew. Chem.* **1994**, *106*, 805–808; *Angew. Chem. Int. Ed. Engl.* **1994**, *33*, 779–781.
[2] H. Furuta, T. Asano, T. Ogawa, *J. Am. Chem. Soc.* **1994**, *116*, 767–768.
[3] K. Berlin, E. Breitmaier, *Angew. Chem.* **1994**, *106*, 1356–1357; *Angew. Chem. Int. Ed. Engl.* **1994**, *33*, 1246–1247.
[4] T. D. Lash, *Angew. Chem.* **1995**, *107*, 2703–2705; *Angew. Chem. Int. Ed. Engl.* **1995**, *34*, 2533–2535.

[5] M. Pawlicki, L. Latos-Grażyński, *Chem. Eur. J.* **2003**, *9*, 4650 – 4660.
[6] S. Venkatraman, V. G. Anand, V. PrabhuRaja, H. Rath, J. Sankar, T. K. Chandrashekar, W. Teng, K. Ruhlandt-Senge, *Chem. Commun.* **2002**, 1660 – 1661.
[7] H. Furuta, H. Maeda, A. Osuka, *J. Am. Chem. Soc.* **2000**, *122*, 803 – 807.
[8] Z. Zhang, G. M. Ferrence, T. D. Lash, *Org. Lett.* **2009**, *11*, 101 – 104.
[9] H. Maeda, A. Osuka, H. Furuta, *J. Am. Chem. Soc.* **2003**, *125*, 15690 – 15691.
[10] T. D. Lash, J. L. Romanic, M. J. Hayes, J. D. Spence, *Chem. Commun.* **1999**, 819 – 820.
[11] S. R. Graham, D. A. Colby, T. D. Lash, *Angew. Chem.* **2002**, *114*, 1429 – 1432; *Angew. Chem. Int. Ed.* **2002**, *41*, 1371 – 1374.
[12] L. L. Xu, T. D. Lash, *Tetrahedron Lett.* **2006**, *47*, 8863 – 8866.
[13] T. D. Lash, D. A. Colby, A. S. Idate, R. N. Davis, *J. Am. Chem. Soc.* **2007**, *129*, 13800 – 13801.
[14] N. Sprutta, M. Świderska, L. Latos-Grażyński, *J. Am. Chem. Soc.* **2005**, *127*, 13108 – 13109.
[15] N. Sprutta, M. Siczek, L. Latos-Grażyński, M. Pawlicki, L. Szterenberg, T. Lis, *J. Org. Chem.* **2007**, *72*, 9501 – 9509.
[16] E. Vogel, W. Haas, B. Knipp, J. Lex, H. Schmickler, *Angew. Chem.* **1988**, *100*, 445 – 448; *Angew. Chem. Int. Ed. Engl.* **1988**, *27*, 406 – 409.
[17] E. Vogel, *Pure Appl. Chem.* **1990**, *62*, 557 – 564.
[18] H. Furuta, H. Maeda, A. Osuka, *J. Org. Chem.* **2001**, *66*, 8563 – 8572.
[19] T. D. Lash, *Synlett* **2000**, 279 – 295.
[20] D. A. Colby, T. D. Lash, *J. Org. Chem.* **2002**, *67*, 1031 – 1033.
[21] W. Haas, B. Knipp, M. Sicken, J. Lex, E. Vogel, *Angew. Chem.* **1988**, *100*, 448 – 450; *Angew. Chem. Int. Ed. Engl.* **1988**, *27*, 409 – 411.
[22] E. Vogel, P. Röhrig, M. Sicken, B. Knipp, A. Herrmann, M. Pohl, H. Schmickler, J. Lex, *Angew. Chem.* **1989**, *101*, 1683 – 1687; *Angew. Chem. Int. Ed. Engl.* **1989**, *28*, 1651 – 1655.
[23] E. Vogel, M. Pohl, A. Herrmann, T. Wiss, C. König, J. Lex, M. Gross, J.-P. Gisselbrecht, *Angew. Chem.* **1996**, *108*, 1677 – 1682; *Angew. Chem. Int. Ed. Engl.* **1996**, *35*, 1520 – 1524.
[24] E. Vogel, C. Fröde, A. Breihan, H. Schmickler, J. Lex, *Angew. Chem.* **1997**, *109*, 2722 – 2725; *Angew. Chem. Int. Ed. Engl.* **1997**, *36*, 2609 – 2612.
[25] T. Asao, S. Ito, N. Morita, *Tetrahedron Lett.* **1988**, *29*, 2839 – 2842.
[26] D. A. Colby, T. D. Lash, *Chem. Eur. J.* **2002**, *8*, 5397 – 5402.
[27] Crystal data for **6-1** an **6-2** are given in the Supporting Information. CCDC 712950 and 712951 contain the supplementary crystallographic data for this paper. These data can be obtained free of charge from The Cambridge Crystallographic Data Centre via www.ccdc.cam.ac.uk/data_request/cif.
[28] S. I. Takekuma, M. Tamura, T. Minematsu, H. Takekuma, *Tetrahedron* **2007**, *63*, 12058 – 12070.
[29] S. Ito, N. Morita, T. Asao, *Tetrahedron Lett.* **1992**, *33*, 3773 – 3774.
[30] S. Ito, N. Morita, T. Asao, *Bull. Chem. Soc. Jpn.* **2000**, *73*, 1865 – 1874.
[31] S. Ito, S. Kikuchi, N. Morita, T. Asao, *Bull. Chem. Soc. Jpn.* **1999**, *72*, 839 – 849.
[32] S. Ito, S. Kikuchi, T. Okujima, N. Morita, T. Asao, *J. Org. Chem.* **2001**, *66*, 2470 – 2479.
[33] S. Ito, T. Kubo, N. Morita, T. Ikoma, S. Tero-Kubota, A. Tajiri, *J. Org. Chem.* **2003**, *68*, 9753 – 9762.
[34] H. Kawai, T. Takeda, K. Fujiwara, K. Suzuki, *J. Am. Chem. Soc.* **2005**, *127*, 12172 – 12173.
[35] K. J. Thorley, J. M. Hales, H. L. Anderson, J. W. Perry, *Angew. Chem.* **2008**, *120*, 7203 – 7206; *Angew. Chem. Int. Ed.* **2008**, *47*, 7095 – 7098.
[36] R. J. Cheng, Y. R. Chen, S. L. Wang, C. Y. Cheng, *Polyhedron* **1993**, *12*, 1353 – 1360.
[37] C. Bleasdale, W. Clegg, S. B. Ellwood, B. T. Golding, *Acta Crystallogr. Sect. C* **1991**, *47*, 550 – 553.

